RF TECHNIQUES FOR $p\bar{p}$

D. Boussard
CERN, Geneva, Switzerland

1. QUASI ADIABATIC MANIPULATIONS IN PHASE SPACE

1.1 Liouville theorem and adiabatic transformations

For hadron machines (no synchrotron radiation), and in the absence of cooling, phase space manipulations are governed by Liouville theorem which states that the six-dimensional phase space volume is conserved. If transverse and longitudinal movements can be separated, which is assumed in the following, then the phase space area, expressed in canonical units: energy and time (unit: eV.s) or $\Delta\beta\gamma$ and phase (unit: mrad), is preserved in any transformation[1].

In many cases the beam before and after the transformation is matched. An intuitive picture of a matched beam is that of a beam having a stationary distribution in phase space, disregarding the individual particles. In other words, along any particular phase space trajectory the local particle density of a matched beam is constant. In the case of a beam with a constant phase space density (often referred to as the "water-bag" model) the beam is entirely defined by its frontier in the phase space diagram. There a matched beam is a beam whose frontier coincides with one particular trajectory.

A beam which is not matched will ultimately grow in macroscopic emittance because of the dependence of synchrotron frequency on oscillation amplitude. For instance, a quasi elliptical unmatched beam will develop long spiralling filaments, giving an extremely complicated frontier after some time (Fig. 1). There is no way to restore the initial situation (except if one could reverse η, which is a very special case), and the final result is a lowering of the average particle density on the edges and therefore an increase of the macroscopic longitudinal emittance: $E_{S2} > E_{S1}$.

This phenomenon has often been compared to the increase of entropy in thermodynamics. Entropy does not grow during adiabatic processes where the equilibrium situation is almost preserved at all times. By analogy, a longitudinal phase space manipulation is called adiabatic if

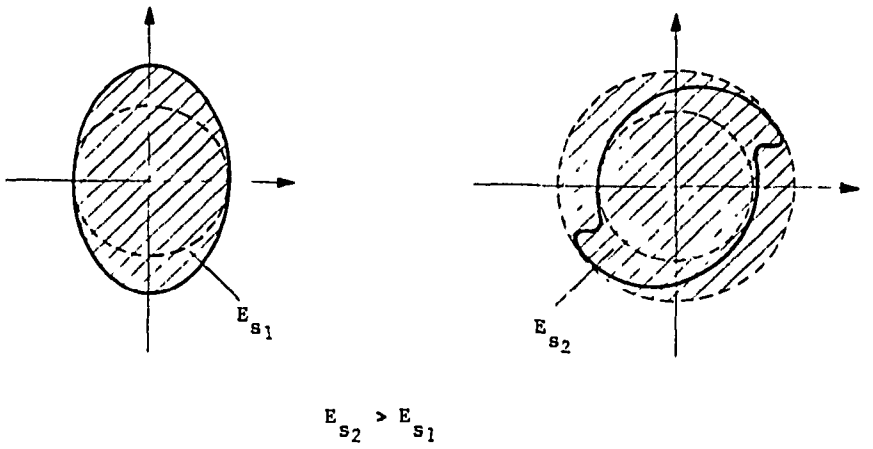

Fig. 1 - Increase of the macroscopic emittance of an unmatched beam by filamentation.

it is slow enough for the beam to stay at equilibrium (i.e. to stay matched) during the whole process. In this case the situation, at the end of the process, is entirely determined by the final bucket parameters and the initial beam emittance. In particular, for a beam having a constant phase space density, the frontier of the beam at the end of an adiabatic manipulation corresponds to the particular trajectory, pertaining to the final values of A and Γ, which encircles the initial beam area E_{s_1}.

What is the meaning of a change of parameters which should be very slow? The typical time scale in the longitudinal phase space is obviously the synchrotron period. Therefore an adiabatic process should be long compared to the synchrotron period. Although this condition is relatively easy to fulfil if one considers particles near the bucket centre, it is never satisfied for particles near the separatrix where the synchrotron period T_S becomes infinite. In this latter case, where the neighbourhood of the separatrix is populated with particles, the process can never be completely adiabatic, hence the name quasi adiabatic.

In the following we ~~shall~~ examine a few typical examples related to proton or antiproton storage rings. (going/HSI)

1.2 Adiabatic trapping

This process refers to the capture of an unbunched beam into stationary RF buckets, at constant average energy ($\Gamma = \sin \phi_S = 0$). At the start of the process the beam is matched (Fig. 2) with $V_{RF} = 0$. This situation corresponds to $T_S = \infty$ and therefore

adiabaticity cannot be perfect. In practice an initial, non zero, RF voltage V_1 is established at the start of the process. V_1 is small enough for the corresponding bucket area A_1 to be much smaller than the initial beam emittance E_{S1} (Fig. 2).

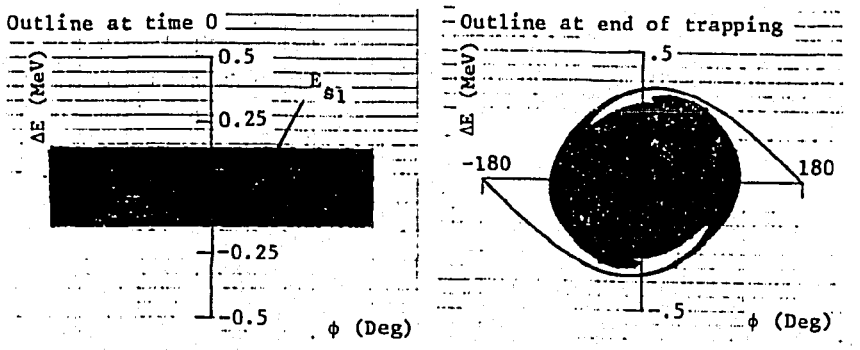

Fig. 2 Adiabatic trappping. iso-adiabatic law

$V_2/V_1 = 12$ $\Delta t/T_{S2} = 2.74$

The adiabaticity coefficient α_c defined, for the trapping process[2,3,4], by:

$$\frac{dA}{A} = \alpha_c \frac{dt}{T_s} \tag{1}$$

should be much smaller than unity (practical values 0.5 to 0.25) for the adiabaticity condition to be approached.

Usually the RF voltage is raised from V_1 to its final value V_2 keeping α_c constant (isoadiabatic law).

As $\Gamma = 0$, $f_s = 1/T_s$ is proportional to A and equation (1) yields:

$$\frac{dA}{dt} = \alpha_c \, k \, A^2 \tag{2}$$

where k is a constant.

Then

$$A(t) = \frac{A_1}{1 - \frac{t}{\Delta t}\left(\frac{A_2 - A_1}{A_2}\right)} \tag{3}$$

A_1, A_2 initial and final bucket areas, Δt duration of the process.

α_c is given by:

$$\alpha_c = \frac{1}{k\Delta t} \cdot \frac{A_2 - A_1}{A_1 A_2} = \frac{T_{s_1} - T_{s_2}}{\Delta t} \qquad (4)$$

Fig. 2 shows the bunch shape obtained with $\alpha_c = 0.9$: matching is not perfect (PSB case)[3].

In the accumulator ring adiabatic trapping is the initial phase of the unstacking process. In order to extract only a fraction of the beam stack (typical value 0.5 eV.s) very low voltages V_1 and V_2 may be required (a few volts in the AA). Reducing the gap impedance is therefore essential. This is achieved by a fast feedback loop built around the RF power amplifier[4].

If the required RF voltage V is impractical (e.g. unstacking for LEAR)[5], one can use a higher harmonic number h. The total bucket area A (all bunches) is given by:

$$A(\text{eV.s}) = \alpha(\Gamma) \frac{16\,\beta}{2\pi f_r} \sqrt{\frac{eV\,E}{2\pi h|\eta|}} \qquad (5)$$

It shows that V and h are inversely proportional at constant A.

With a broad-band RF system, it is even possible to generate a single sine wave (frequency $h\,f_r$) per turn (Fig. 3). In this case (isolated bucket technique) V is proportional to h^{-3} at constant A. Unstacking for LEAR will use the cooling kickers as a wide-band cavity (250-500 MHz) working on h = 128 [5]. Only 10 buckets out of 128 will be energized during capture.

The isolated bucket technique can also be used to preserve a gap in a coasting beam, even during cooling[6]. The "barrier" is obtained by reversing the phase of the RF waveform (Fig. 3).

1.3 Phase displacement

Consider an unbunched stack of particles and a stationary bucket (empty) far away from the stack. This is a quasi-equilibrium situation as the trajectories far from the bucket are almost parallel to the phase axis (Fig. 4). What happens if we start to move the bucket through the stack by changing the RF frequency?

At constant $\Gamma = \sin \phi_s$ and constant A, the initially empty bucket remains empty during the traversal of the stack. This is a consequence of Liouville theorem: if the bucket were full of particles, all those particles would remain inside (at constant Γ and constant A),

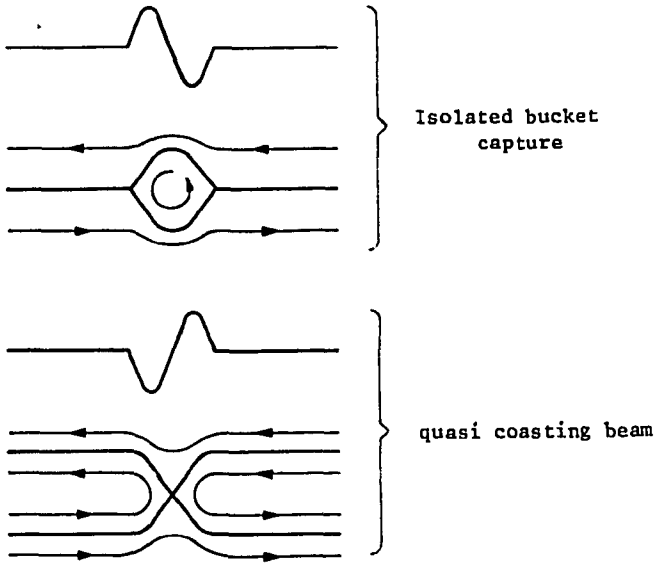

Fig. 3 - Isolated bucket techniques.

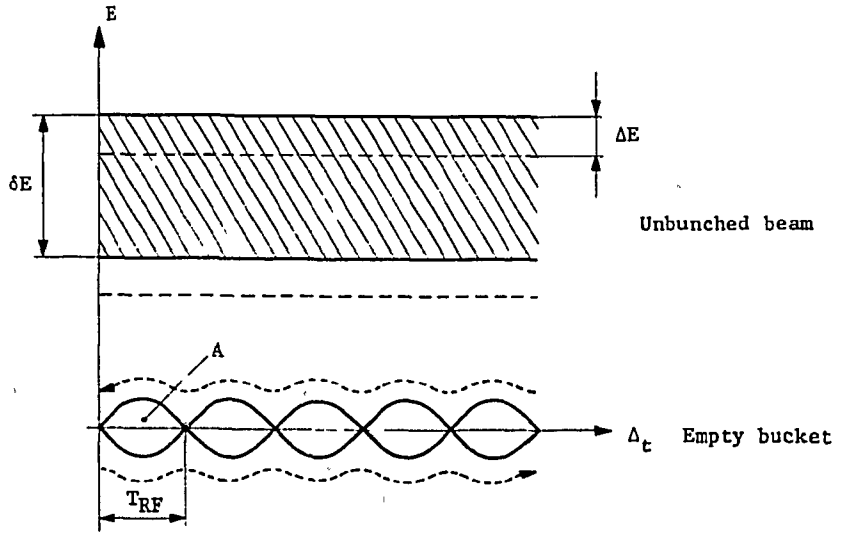

Fig. 4 - Phase displacement.

and therefore, if outside particles were to penetrate inside the bucket, the local density would then increase, which is in contradiction with Liouville theorem. Contrary to the adiabatic trapping case (increasing A), no particles are captured by the empty bucket.

If the bucket sweeps the stack very slowly ($\Gamma \ll 1$; in practice $\Gamma \simeq 0.2$) adiabaticity is almost preserved and the stack is again almost at equilibrium after the traversal, with the same energy spread δE. As phase space area is incompressible (Liouville theorem) the upwards displacement of the empty bucket results in a downwards movement of the stack by an amount $\Delta E = A/T_{RF}$ (phase space conservation)[7].

A more elementary explanation of this result is given in the following. During the traversal, the empty bucket immersed in the stack produces an RF beam current opposite to that produced by a full bucket (having the same density ψ) in empty space. Therefore the energy exchanges between RF cavity and beam are just opposite in these two situations.

The energy gained by the beam W_1 (full bucket case) when accelerated by δE writes:

$$W_1 = \psi \, A \, \delta E \tag{6}$$

where ψ is the number of particles per unit area.

The energy lost by the stack, W_2 (empty bucket case), decelerated by ΔE is given by:

$$W_2 = \psi \, T_{RF} \, \delta E \, \Delta E \tag{7}$$

The relation $W_1 = W_2$ gives:

$$\Delta E = \frac{A}{T_{RF}} \tag{8}$$

By passing an empty decelerating bucket through the stack, acceleration is achieved. This method, repeated many times, is used in the ISR to bring, with small bucket size, the stack energy up to 31 GeV/c[8,9] (phase displacement acceleration). By measuring the RF beam current during the traversal, one can also obtain the energy profile of the beam[10]. This is best done with a high harmonic number (RF scanning technique)[11].

1.4 Beam deposit

If, instead of being empty, the bucket moving through the stack is full of particles, these can be carried inside the stack and deposited there (AA filling, for instance).

If the stack and bucket densities are equal and constant the moving bucket is simply switched off in the middle of the stack: the new particles will fill up the space left by phase displacement of the traversed part of the stack.

In the case of more realistic density distributions in the stack (increasing density from the tail to the core) and in the bucket (dense core, lower density near the separatrix), it is more interesting to combine the moving bucket technique and shrinking of the bucket size (inverse of adiabatic trapping)[4]. This brings the denser core of the bunch furthest inside the stack (region of higher density), leaving the less dense outer particles in the tail of the stack distribution. Best matching is achieved in this way.

The typical case is when the phase space area traversed by the bucket equals the reduction in bucket area:

$$\frac{dA}{dt} = \frac{dE}{dt} \cdot T_{RF} = \frac{\Gamma\, eV}{h} \qquad (9)$$

At constant Γ, eV is approximately proportional to A^2, and equation (9) is similar to (2) and yields similar functions A(t), V(t) and f(t).

1.5 Adiabaticity in the case of two RF frequencies

Consider a bunched beam held in an RF bucket generated by the RF voltage V at frequency f_1. If, in the same ring we superimpose a second RF voltage (amplitude V, frequency f_2), the effect on the beam will be small if $|f_2 - f_1|$ is large, because there will be no synchronism between the beam and the second RF waveform. One can also represent the superposition of frequencies f_1 and f_2 by a phase and amplitude modulation of waveform f_1 at a frequency $|f_2 - f_1|$. When $|f_2 - f_1|$ is of the order of f_s (synchrotron frequency) the adiabaticity condition is far from being fulfilled and strong distortion of the bunches will occur. However, for larger and larger values of $|f_2 - f_1|$ the effect on the beam of frequency f_2 will become smaller and smaller and the behaviour of the bunch will become independent of the second RF waveform. The same would be true for a beam initially held by the RF frequency f_2.

Consequently, for $|f_2 - f_1| \gg f_s$ two beams can be kept simultaneously bunched in the same machine although the instantaneous parameters seen by each beam are rapidly varying functions of time.

Theoretical arguments[12] have led to the independence condition $|f_2 - f_1| > 4\ f_s$, but this is not a sharp limit as shown in Fig. 5[13].

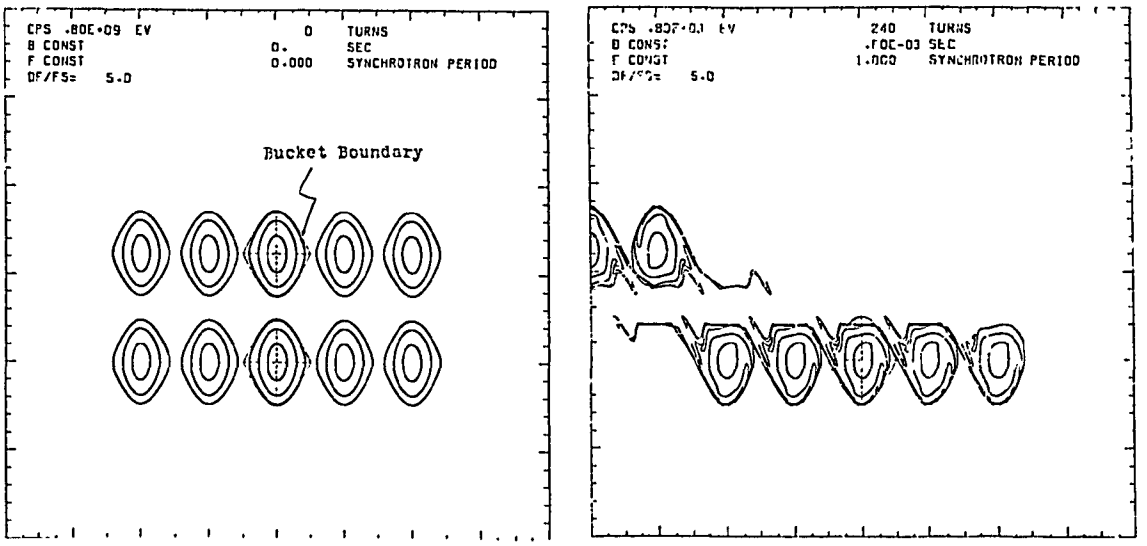

Fig. 5 - Phase space trajectories in the case of two RF frequencies $|f_2 - f_1| = 5\ f_s$.

Independent control of two beams in the same machine by two RF frequencies has found an application in the CPS at 26 GeV, where two sets of five bunches are drifting in azimuth at the frequency $|f_2 - f_1|/h$. Doubling of the local intensity is achieved when the two sets of bunches merge: the beam is then extracted and sent onto the target for antiproton production[13,14].

It is interesting to note that if $|f_2 - f_1| = f_r$, the modulation is synchronous with the beam revolution frequency, like in the case of the isolated bucket technique. Several cavities working on different harmonic numbers can therefore be used to synthesize a pseudo-isolated bucket[14].

2. BUNCH ROTATION TECHNIQUES

2.1 Quarter-turn rotation in phase space

Consider the usual case of bunch transfer from one machine to the next. At $\Gamma = 0$, matching is always possible in theory by properly adjusting the RF voltages in the two machines. Superposition of the two families of trajectories is obtained (at low amplitudes) for:

$$\frac{h_1 V_1}{n_1} f_{r_1}^2 = \frac{h_2 V_2}{n_2} f_{r_2}^2 \qquad (10)$$

This situation may also happen in a single machine when the harmonic number is changed (example of the CPS at 3.5 GeV where a change of h = 20 to h = 6 is performed).

In many cases the matching voltages may turn out to be prohibitive or impractical. Bunch rotation techniques often offer a more economical solution to the problem.

Take the example of a matching voltage V_2 in the receiving machine which is too small to be practical. The beam is injected mismatched (voltage $V_0 > V_2$) and is left to rotate for a quarter of a turn in phase space (Fig. 6) at constant voltage V_0. The voltage is then abruptly raised to the final value V'_2 which matches the upright ellipse.

This simple technique works for beams with a small enough emittance such that the synchrotron oscillation can be considered as linear. The RF voltages are such that:

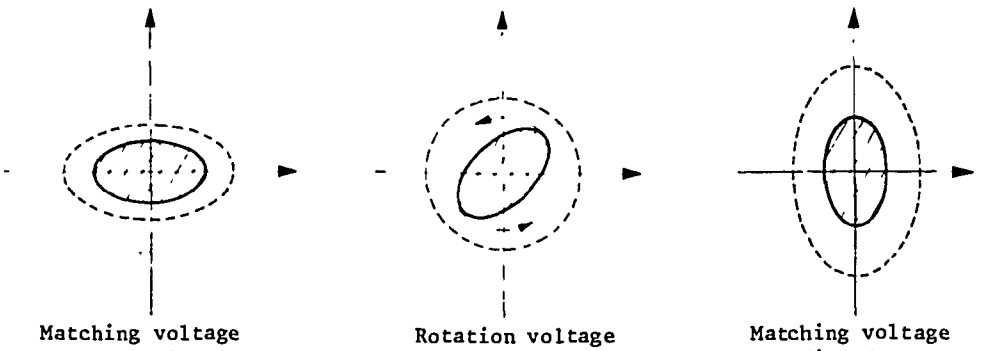

Fig. 6 - Matching by 1/4 turn rotation.

$$V_o^2 = V_2 \, V'_2 \qquad (11)$$

(similar to the impedance relation for a $\lambda/4$ transformer in radiofrequency technique).

Bunch rotation is a common technique[15]; to avoid bunch distortions it requires a fast control of the RF amplitude.

2.2 180° phase jump

The mismatch prior to rotation in phase space can be very conveniently obtained by letting the beam sit for some time on the unstable fixed point in the phase space diagram (RF phase jump of 180° at $\Gamma = 0$). The degree of mismatch obtained depends on how long the beam is kept on the unstable fixed point (Fig. 7). When the RF phase is

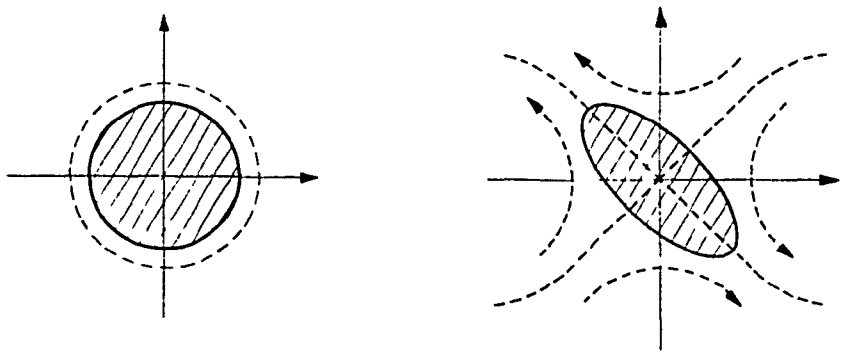

Fig. 7 - 180° phase jump

brought back to its original value, the mismatched beam rotates around the stable fixed point. When its length is maximum (or minimum) the bunch is transferred (or recaptured by another RF system).

This technique is very popular because it does not require a fast change in RF voltage amplitude, but only a phase jump easy to generate in the RF low-level circuits.

Again, this method is limited to small bunches inside large buckets, because the non linearity of the synchrotron motion (around either the stable or the unstable fixed points) rapidly distorts the bunch shape. It is interesting in this respect to use a low value of h which provides larger buckets for a given RF voltage. For instance, in the CPS the proton and antiproton bunches are accelerated from 3.5 GeV to 26 GeV on h = 6 (lower frequency limit of the RF system) to provide a larger bucket

for bunch rotation at 26 GeV/c. This in turn requires a change of harmonic number on the 3.5 GeV intermediate flat top for the protons (from h = 20 to h = 6).

2.3 Use of an harmonic cavity

To limit the bunch shape distortion one can envisage linearizing the RF voltage, especially during bunch rotation. This can be partially achieved by using an harmonic cavity working at a multiple of the RF frequency. In the bunch compression operation at 26 GeV in the CPS two sets of cavities (h = 6 and h = 12) are used for this purpose[16].

As the linear part of the RF wave is only needed along the phase extension of the bunch, (which varies considerably during the rotation) optimum use of the equipment is obtained with a varying slope, constant amplitude RF waveform[16]. The results for the 26 GeV bunch compression in the CPS are displayed in Fig. 8. With very high compression ratios like those achieved in the CPS (20 ns → 4 ns), the final phase jitter of the ejected bunch may become a problem. In particular, following the CPS experience, phase loops had better be disconnected during bunch compression.

2.4 Bunch rotation for antiproton production

The useful energy spread of the antiprotons produced at the target is fixed by the momentum acceptance of the transfer channel. Therefore maximum density of the antiproton bunches is obtained by minimizing the incoming proton bunch length at constant intensity (for instance by using the bunch compression technique described in 2.2)[15].

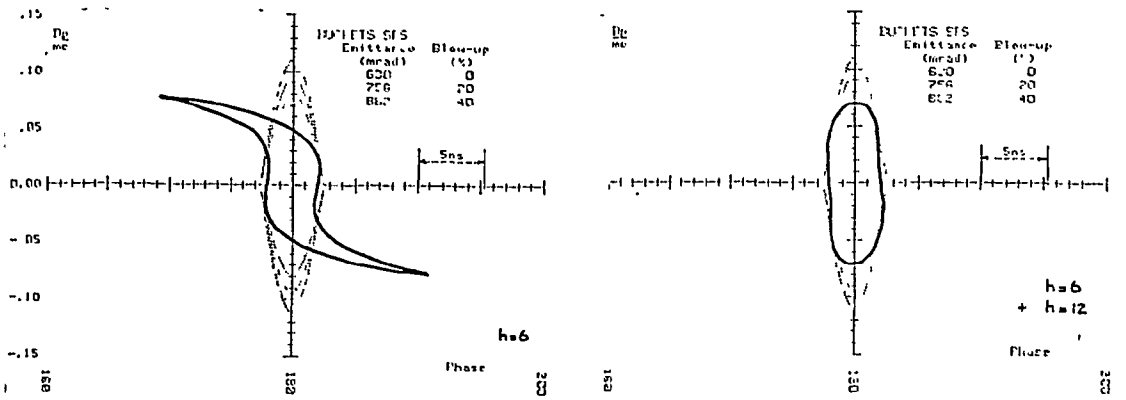

Fig. 8 - Use of an harmonic cavity in the CPS.

To make best use of the maximum antiproton density in a cooling ring the short antiproton bunches, having a large δE could be rotated by one quarter of a turn in phase space to give (ideally) a coasting beam with a much smaller energy spread.

It is conceivable to achieve this rotation between the target and the cooling ring, if a very high frequency bunching is present on the proton beam, and if very high RF voltages (e.g. obtained with a pulsed linac structure) are available. However, the favoured solution at present is to use an intermediate ring (debunching ring at FNAL, ACOL at CERN[17]) having a large momentum acceptance and where bunch rotation is performed with a pulsed cavity (pulse length = $^1/_4$ T_s). The conflicting requirements for this cavity are large voltage (high Q) to accept as much energy spread as possible and a fast decay (low Q) to quickly empty the cavity after the bunch rotation[18].

3. LOW LEVEL RF SYSTEMS

3.1 RF amplitude and frequency controls

Even in the cases where beam loading is negligible (e.g. antiproton beams), the RF amplitude is regulated by a servo-system (usually called A.V.C. or A.G.C.). The RF amplitude (preferably measured at the gap) is compared to a given reference and acts through a loop amplifier on the modulator inserted in the RF drive line (Fig. 9). Gain and bandwidth of the servo loop are limited by the unavoidable delays and the Q of the cavity.

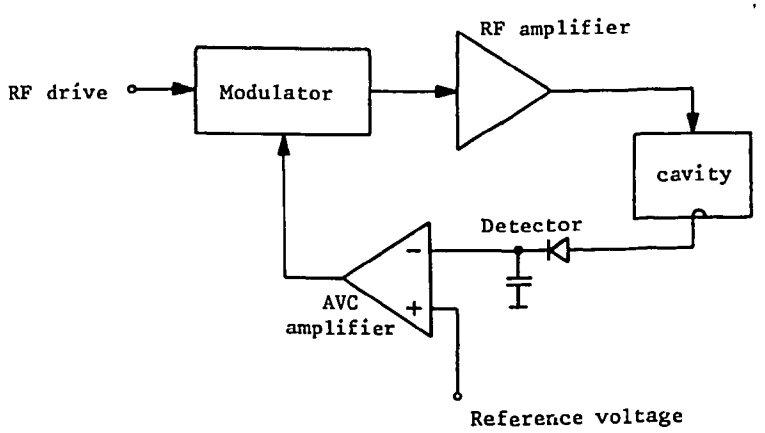

Fig. 9 - Amplitude control of RF voltage.

When a large dynamic range (> 60 dB) is required (this is the case for the AA) the detector and modulator are of the logarithmic type[4]. For a machine having several RF cavities, the RF amplitude can be controlled by outphasing the RF drive signals of each cavity. The advantage is that multipactoring effects at low RF fields in the cavities can be avoided. On the other hand, phase noise in the outphasing circuitry is transformed into amplitude noise seen by the beam.

The RF frequency is, in most cases, generated by a voltage-controlled oscillator (V.C.O.). The voltage applied to its input depends on the particular operation to be performed; it can, for instance, be:

- a frequency programme derived from a measurement of the bending magnetic field for particle acceleration,
- an off-line calculated function for RF stacking or unstacking,
- a phase detector voltage for RF synchronization between two machines (phase locked loop).

Note that the classical control of the RF frequency by a measurement of the beam radial position, which is difficult to make completely insensitive to beam intensity, is in most $p\bar{p}$ schemes replaced by a calculated frequency programme, derived from B field measurement.

Although the radial error becomes theoretically infinite at transition in a frequency-controlled system, acceleration through transition is nevertheless possible if the errors of the frequency programme are very small and if the crossing is made fast enough. This is the case in the CPS for proton and antiproton acceleration, where the γ_{tr} jump is used even for very low intensity beams.

Stability and precision of the RF frequency are better achieved with a frequency synthesizer in the locked mode. On the other hand analog V.C.O.'s provide fast speed and low noise (absence of switching transients). In most RF low-level designs one uses a combination of a very stable frequency synthesizer and a fast analog VCO.

Single side band mixing can be used to generate the sum (or difference) frequency from two quadrature generators: synthesizer and small frequency range VCO (Fig. 10). This is the system used in the AA[4].

Another solution is to use a frequency loop (CPS, SPS) sketched in Fig. 11, where the low frequency drifts of the analog VCO are corrected by a slow servo system[19].

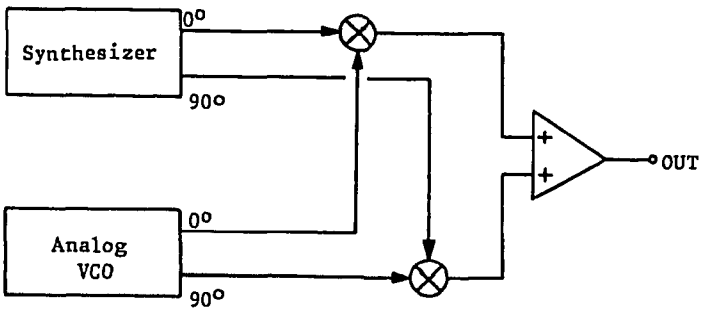

Fig. 10 - Schematics of a single sideband mixer (SSB).

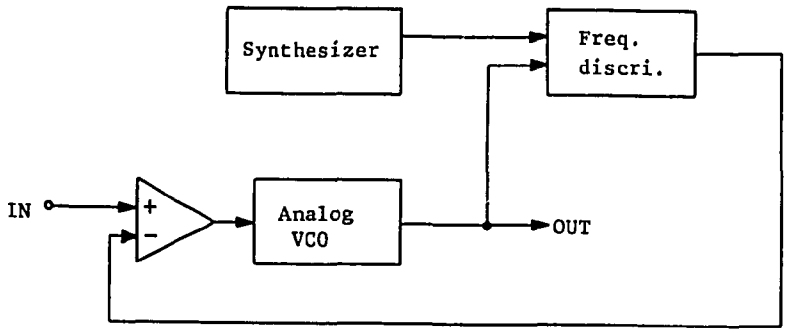

Fig. 11 - Correction of slow drifts by a frequency loop.

3.2 Damping loops

The RF low level systems described in 3.1 are perfectly adequate for short time periods, for instance during the initial part of adiabatic trapping or during bunch rotation. On the other hand, to keep the beam for very long times, like in the collider, it is absolutely essential to provide damping against slowly growing instabilities, RF or magnet noise excitation, or even injection phase and energy errors. In hadron machines, where damping of individual particles is absent, this is achieved by supplementary loops taking information from beam measurements.

Beam oscillations, which can be decomposed into normal modes[20], dipole, quadrupole etc., are detected by pick-up electrodes and the signals used to correct the RF waveform sent to the cavities. Dipole oscillations are damped by the usually called phase loop, whereas the quadrupole damping loop suppresses quadrupole mode oscillations.

Although damping of modes higher than quadrupole may be necessary in very high intensity machines (e.g. PS Booster), it seems sufficient for $p\bar{p}$ operation to damp dipole and quadrupole modes only.

In the case of the SPS collider the quadrupole loop is only needed to stop slowly growing instabilities, and therefore its modest gain does not appreciably change the RF amplitude noise seen by the beam. On the contrary, the large gain of the main phase loop is essential to suppress the phase noise of the V.C.O.

Dipole oscillations are detected by measuring the phase difference between the RF component of the bunch and the RF waveform seen by the bunch itself (gap voltage in the case of a single cavity, vector sum of all gap voltages if several cavities are used). Damping is achieved if this signal is phase shifted by 90° (at frequency f_s) and used to correct the RF gap phase[21,22].

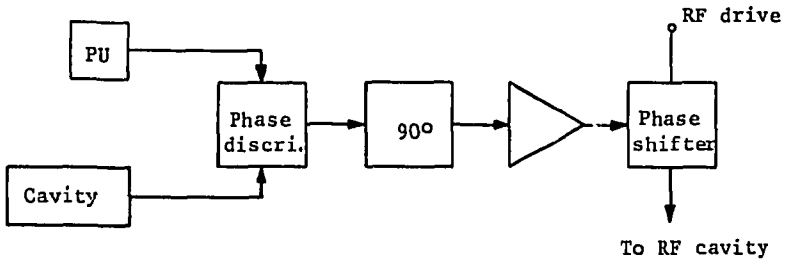

Fig. 12 - Dipole damping loop.

Fig. 12 is a sketch of such a dipole damping loop. The quadrature at f_s can be obtained by a low pass network. To avoid large phase excursions on the phase shifter at large gains, AC coupling may be used. By adding multiplexing circuits (synchronized with the bunch repetition frequency) at the phase discriminator level and at the phase shifter level, independent damping of several bunches is possible, provided the cavity bandwidth is sufficient (SPS).

In a very common design (Fig. 13) the necessary quadrature is obtained by frequency to phase conversion. The loop amplifier (gain G_p) may be AC coupled as a large gain is only needed in the neighbourhood of f_s. DC gain can also be used in conjunction with a frequency loop (Fig. 11). In fact, in this configuration the VCO input (with frequency loop included) is almost AC coupled as slow signals are compensated by the frequency loop itself.

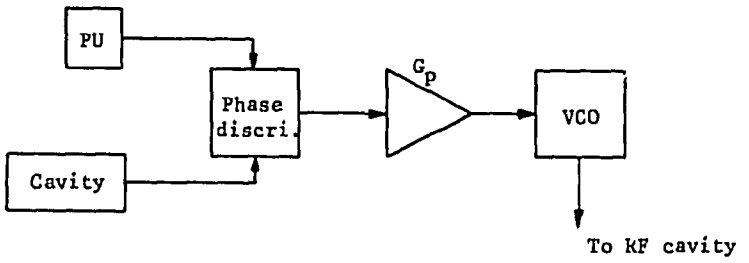

Fig. 13 - Dipole damping loop acting on the VCO directly.

Note that, if the frequency loop is replaced by a phase lock loop (in order to synchronize two RF systems, for instance), the DC coupled dipole loop will become unstable (two integrators in cascade). A phase advance network is then necessary in the phase-locked loop (also called synchronization loop).

Quadrupole oscillations result in a modulation of the line density of the bunch which is easily detected by a wide-band electrode followed by a peak detector. Again, quadrature at $2 f_s$ [23] is necessary to achieve damping, like in Fig. 12 (usually with a high pass filter). The signal is reinjected into the AVC circuits of the cavity to modulate the RF amplitude.

4. ANALYSIS OF RF NOISE SEEN BY THE BEAM

4.1 Single bunch case

We shall take in the following the example of the SPS collider: the first injected proton bunch is the reference bunch for the DC coupled phase loop (Fig. 13). For that particular bunch, the RF low level system of Fig. 14 (including the frequency loop of Fig. 11) can be represented by the small signal flow diagram of Fig. 15 where the phase noise sources u are independent random signal generators[19,24].

- u_r is the frequency noise of the combination: reference oscillator (synthesizer) and frequency discriminator
- u_F is the frequency noise of the VCO and the RF power amplifier
- u_m is the magnetic field noise
- u_p is the phase discriminator noise (referred to its output).

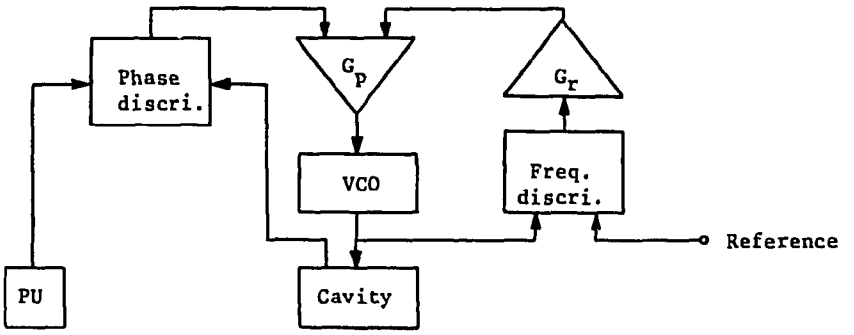

Fig. 14 - Schematics of the RF low level system of the SPS (main phase loop and frequency loop).

To be more precise, the quantities u_f and u_p represent the low frequency signals obtained by periodic sampling at f_r of the actual random waveforms (whose frequency spectra may extend much beyond f_r).

$G_r(\omega)$ and $G_p(\omega)$ are the gains of the frequency loop (frequency → phase) and the phase loop (phase → frequency) respectively.

$B(\omega)$ is the beam transfer function which relates the beam-RF phase difference to the RF frequency deviation.

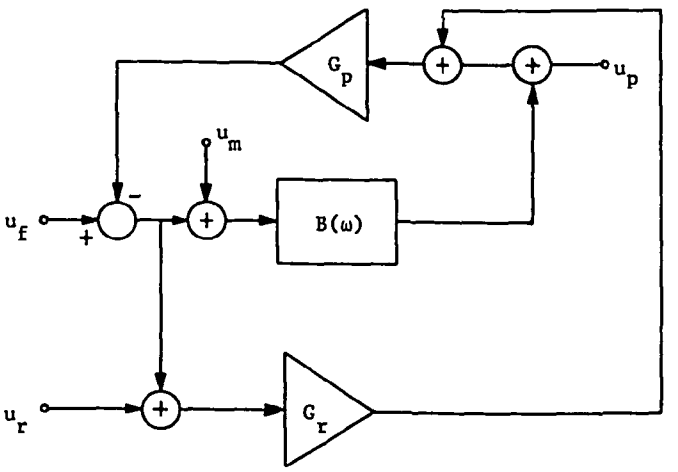

Fig. 15 - Equivalent small signal flow diagram of Fig. 14.

In the limit of zero frequency spread:

$$B(\omega) = \frac{j\omega}{\omega_s^2 - \omega^2} \tag{12}$$

has a pole at $\omega = \omega_s$.

$B(\omega)$ is related to the bunched beam dispersion integral[25] and is represented in the complex plane by a curve following the imaginary axis except for frequencies ω within the band of the incoherent synchrotron frequencies of the bunch (Fig. 16). Inside this band $|B(\omega)|$ is of the order of $1/s$ where s is the synchrotron frequency spread[25].

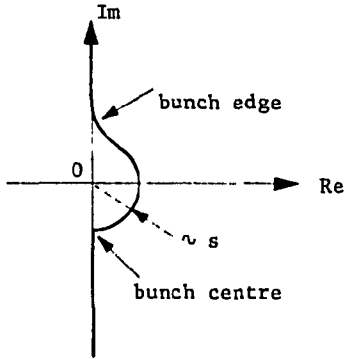

Fig. 16 - Beam transfer function in complex plane.

From Fig. 15 we calculate y, the frequency noise seen by the beam, and the measurable phase discriminator output u. For simplicity, u_m has been included in u_f.

$$y = \frac{u_f + G_p G_r u_r + G_p u_p}{1 + G_p(B + G_r)} \tag{13}$$

$$u = \frac{B(u_f + G_p G_r u_r) + u_p(1 + G_p G_r)}{1 + G_p(B + G_r)} \tag{14}$$

For the unrealistic case $s = 0$, one finds $u = (u_f + G_p G_r u_r)/G_p$ and $y = 0$ at $\omega = \omega_s$. The phase (or frequency) noise spectral density at ω_s vanishes because the loop gain becomes infinite at the pole, and consequently there is no diffusion.

For $s \neq 0$, we must evaluate the various terms in (13) and (11) according to the measured transfer functions G_p and G_r.

If we neglect u_p for the moment, Equations (13) and (14) give:

$$y \simeq \frac{u}{B} \tag{15}$$

The noise measured at the output of the phase discriminator is proportional to the frequency noise seen by the beam. We can distinguish two regions:

- at very low frequencies the contribution of u_r dominates because G_p and G_r are large and $y \simeq u_r$.
- at high frequencies u_f is the dominant term and the observed signal $u \simeq u_f/G_p$ is the same whether the phase loop is locking the RF onto the beam or onto an external RF generator (at high frequency, $\omega >> \omega_s$, the beam is completely rigid and equivalent to an external generator).

For the contribution of u_p, Equation (15) does not hold, and in the region of interest where B is large, we find:

$$y \simeq u_p/B \tag{16}$$

and

$$u \simeq u_p/B\ G_p \tag{17}$$

Unless u_p is very large, it does not appear on the measured signal u because the quantity BG_p is much larger than unity. On the other hand, Equation (16) is identical to Equation (15) if we replace u_p by u.

The conclusion is that the noise seen by the beam cannot be directly measured at the phase discriminator output, unless u_p is deliberately increased (Fig. 17 [25]). Note that from the measured spectrum of u, one can determine $|B(\omega)|$.

The quantity u_p must be determined by independent measurements.

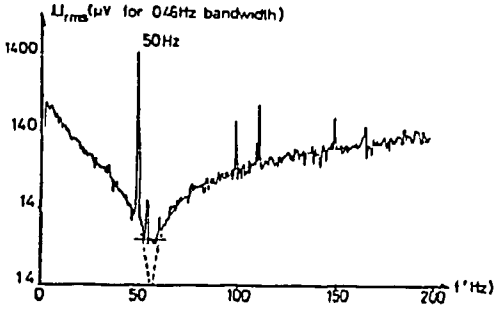

Fig. 17 - Spectrum of u (proportional to $1/|B|^2$) with white noise added (ISR).

4.2 Phase discriminator noise

The phase discriminator measures the phase difference between the RF voltage in the cavity and an RF burst excited by the passage of the bunch in a pick-up electrode followed by a band pass filter.

If the filter bandwidth δ_f is very small (~ bunch repetition frequency) the beam signal is almost a continuous wave, but with a small amplitude. From the noise point of view, it is better to keep a short RF burst and to sample the phase detector output at the revolution frequency (Fig. 18). The noise level increases as $\sqrt{\delta f/f_r}$, but the signal is proportional to $\delta f/f_r$.

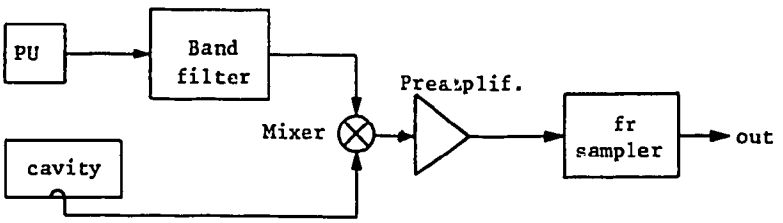

Fig. 18 - Phase discriminator for the SPS collider.

In the SPS case ($\delta f \simeq 5$ MHz), the preamplifier noise (calculated equivalent noise figure ~ 8 dB) seems to be the dominant source of noise in the phase discriminator circuitry. The measured value of u_p is ~ $1.6\ 10^{-6}$ rad/√Hz (laboratory measurement); the frequency spectrum is flat except at very low frequencies (Fig. 19) [19].

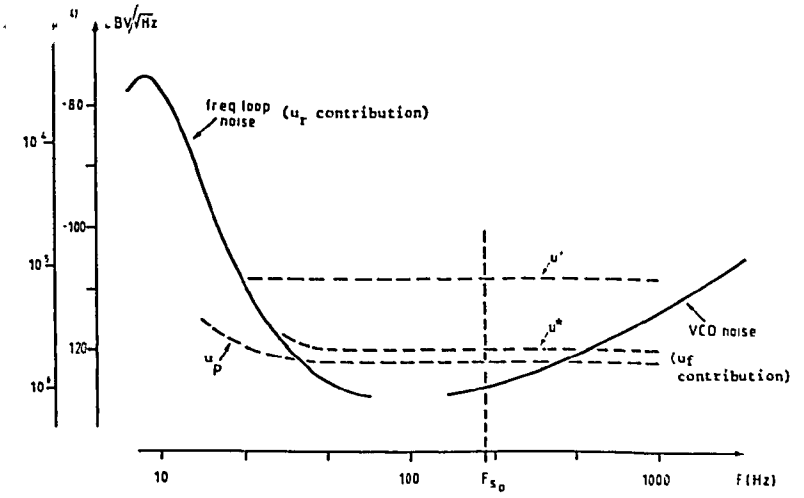

Fig. 19 - Noise levels measured in the SPS RF system.

The quantity u_p can also be measured with the real beam signals if a second phase discriminator, identical to that in use in the phase loops, is available. The second phase discriminator, installed in parallel with the operating one (possibly using a different PU electrode) delivers a voltage $u^* \simeq \sqrt{2}\ u_p$, in the frequency range where $u \ll u_p$, if the noises of the two detectors are uncorrelated (Fig. 19).

For a well-designed low-level system, the phase discriminator should be the ultimate element to determine y in the frequency range of interest, i.e. in the neighbourhood of f_s: $y \simeq u_p/B$. By a careful choice of parameters G_A and G_p, the other contributions which may involve power equipment can, in principle, be made negligible around f_s.

Phase discriminator noise, which is the ultimate source of phase noise seen by the beam, can easily be spoiled if the RF signal coming from the RF cavities to the discriminator does not exactly represent what the beam actually sees.

In the case of several RF cavities the reconstruction of the RF vector sum from the gap voltages may be imperfect. Then u_f contributes to u_p; measurements with only one cavity can be used to evaluate this effect. The delays pickup electrode-phase discriminator and cavity-phase discriminator should be such that the part of the RF waveform present when the bunch passed through the cavity is actually compared to the beam phase in the discriminator. Otherwise the high frequency contribution in u_f will also spoil u_p. This would also be the case if the phase discriminator averages the cavity RF phase over a time longer than the

time determined by the bandwidth of the power amplifier-cavity combination. This condition imposes a lower limit on the bandwidth of the preamplifier in front of the sampling circuit (Fig. 18).

4.3 Multibunch case

For the low frequency ($<< f_r$) contributions to the noise sources in Fig. 15 the situation is the same for all bunches. However, the noise components around n f_r ($n \neq 0$) in u_f combine differently for the various bunches. Only for the first bunch are these components corrected by the phase loop, for the others they appear as VCO noise in a system without phase loop. The equivalent phase noise obtained by sampling high frequency (n f_r) noise components of the VCO has a flat spectrum (as $f_s << f_r$), consequently the equivalent frequency noise source u'_f has a spectral density proportional to ω^2.

This result emphasizes the importance of VCO and RF power amplifier noise at large offset frequencies. For the SPS, one uses a specially-designed VCO[26], having very low noise far away from the carrier (Fig. 20).

Separate dipole damping loops working on each bunch can be used to reduce the effect of the "high frequency" VCO noise. They could conveniently use the design of Fig. 12, but with a much smaller gain G_p' than the main phase loop, as the "high frequency" VCO noise (even sampled) is considerably smaller than the "low frequency" component.

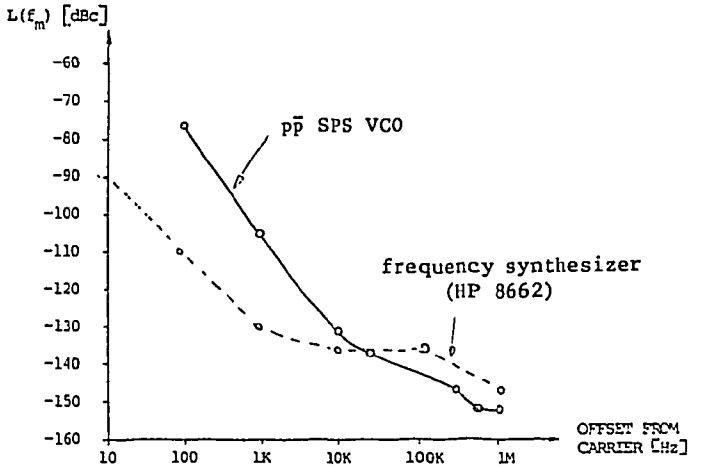

Fig. 20 - Phase noise performance of $p\bar{p}$ VCO
(stabilized against drifts by temperature control).

For the now dominant noise source u'_f we find:

$$y' = \frac{u_f'}{1 + G'_p B} \quad \text{frequency noise seen by the beam} \tag{18}$$

$$u' = \frac{B\, u_f'}{1 + G'_p B} \quad \text{measured noise on phase discriminator output} \tag{19}$$

$$y' = \frac{u'}{B} \tag{20}$$

The RF noise seen by bunches other than the first is directly related to the measured spectrum of u' (Fig. 19).

There is no difference between proton and antiproton bunches if standing wave cavities are used. However, proton and antiproton beams do not see the same RF waveform in the case of directional cavities like the travelling wave structures in the SPS. There, even the "low frequency" noise components of the antiproton cavities circuitry are not corrected by the main phase loop, working on a proton bunch. The analysis is exactly the same as before, u'_f now including noise components at low frequency. u'_f is easily determined by measuring the output signal u' of the antiproton phase discriminator and y' is obtained by Equation (20).

5. RF NOISE EFFECTS ON THE BEAM

5.1 Emittance growth rate

The evolution of a single particle oscillation amplitude, when submitted to RF noise, is governed by the relation: (RF theory part)

$$\left\langle \frac{\Delta x}{\Delta t} \right\rangle = \frac{\omega_s^2}{4} \left[S_\phi (\omega_s) + 2x\, S_a(2\omega_s) \right] \tag{21}$$

where $\langle\ \rangle$ denotes an ensemble average over all possible noises having the spectral density S_ϕ (phase noise) and S_a (amplitude noise), and the quantity

$$x \approx \sin^2 \frac{\hat{\phi}}{2}$$

goes from 0 in the centre to unity on the separatrix. ($\hat{\phi}$ is the phase oscillation amplitude).

For many particles, submitted to the same sample of RF noise, the synchrotron frequency spread destroys the coherence between the particles on a sufficiently long time scale, . Therefore, the average over possible noise samples can be replaced by an average over particles in

the bunch. For this to be valid we assume sufficiently small perturbations and sufficiently long time scales, such that the beam always remains matched. This is a situation exactly analogous to that found in momentum spread cooling theory: coherence is always lost by mixing between particles, only the energy information is retained.

Not all particles may be submitted to the same sample of RF noise. This is the case, for example if an harmonic cavity is used and there exists phase noise between the two RF systems. There the need for small perturbations and long time scales is greatly reduced and clean emittance blow-up can be obtained much faster (example of the CPS controlled blow-up at 1 GeV/c [27]).

The conclusion is that, for small amplitudes, x is a quantity proportional to E_s (for a given bucket): the evolution of longitudinal beam emittance results from Equation (21).

S_a is directly measurable on the cavity gap, but as we have seen in the previous chapter S_ϕ is more difficult to evaluate. It is related to the spectrum of y (frequency noise) by:

$$S_\phi(\omega) = \frac{1}{\omega^2} S_y(\omega) \tag{22}$$

For a given electronic noise (u_p, u_f, u_r), y is proportional to 1/B (Equations 15, 16, 20). In the band of particle synchrotron frequencies we approximate 1/B by s [28] and obtain:

$$S_\phi(\omega_s) = S_u \, s^2/\omega_s^2 \tag{23}$$

S_u being the "electronic" noise spectral density.

In a stationary bucket s/ω_s is proportional to ϕ^2, hence Equation (21) becomes, for phase noise only:

$$\left(\frac{\Delta x}{\Delta t}\right) = k'x^2 = k' \frac{\omega_s^2}{4} S_u(\omega_s)x^2 \tag{24}$$

with the solution:

$$x(t) = \frac{x_i}{1 - k x_i t} \tag{25}$$

represented in Fig. 21. Experimental results[28] are displayed in Fig. 22.

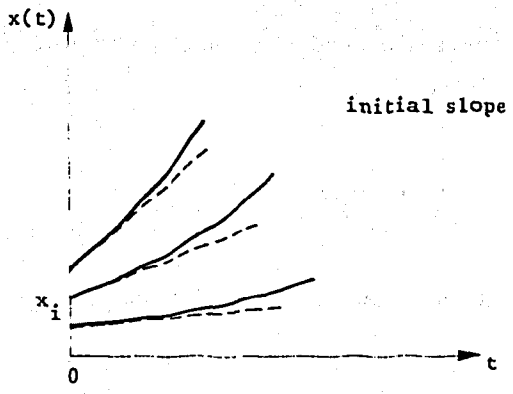

Fig. 21 - Evolution of x(t) or E_s for various x_i.

To minimize the initial slope (k x_i^2):

- minimize k' by using an harmonic cavity to linearize the RF waveform[28]. This is at the expense of Landau damping and more feedback systems may become necessary.

- minimize x_i. At constant E_s, x can be minimized by raising the RF voltage (x_i^2 proportional to 1/V). However, ω_s^2 goes like V and the growth rate depends on the particular shape of $S_u(\omega)$.

- minimize k by reducing the "electronic" noise level is a much more economical solution.

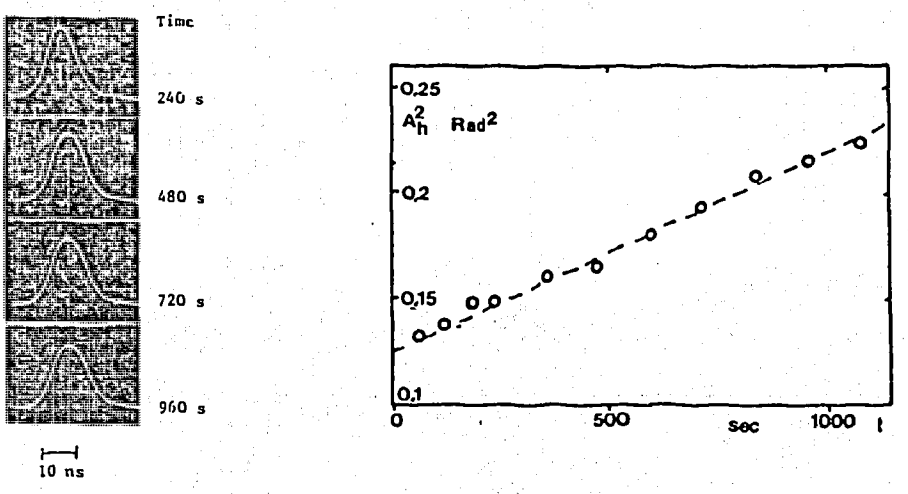

Fig. 22 - Emittance growth in the ISR (bunched beam).

5.2 Equilibrium distributions

Long term evolution of a bunch submitted to RF noise is obtained by solving the diffusion equation:

$$\frac{\partial \rho}{\partial t} = \frac{\partial}{\partial x}\left[\frac{\omega_s^2}{4}\left(x\, S_\phi\,(x) + x^2\, S_a(x)\right)\frac{\partial \rho}{\partial x}\right] \qquad (26)$$

with the boundary condition $\rho(x = 1) = 0$ on the separatrix. The solutions having the slowest decay determine the equilibrium distribution and the equilibrium life time τ_{eq}.

In the case of amplitude noise, where the weak quadrupole damping loop perturbs the amplitude noise spectrum of the RF voltage very little, the model of a constant noise spectral density S_a is adequate.

τ_{eq} is given by (RF theory part):

$$\tau_{eq} = 16/(\omega_s^2\, S_a(2\omega_s)) \qquad (27)$$

This relation has been verified in the SPS by deliberately injecting white noise into the cavity A.V.C. circuits (Fig. 23).

For phase noise, $S_\phi(x)$ depends on the equilibrium distribution itself which determines the beam transfer function $B(\omega)$.

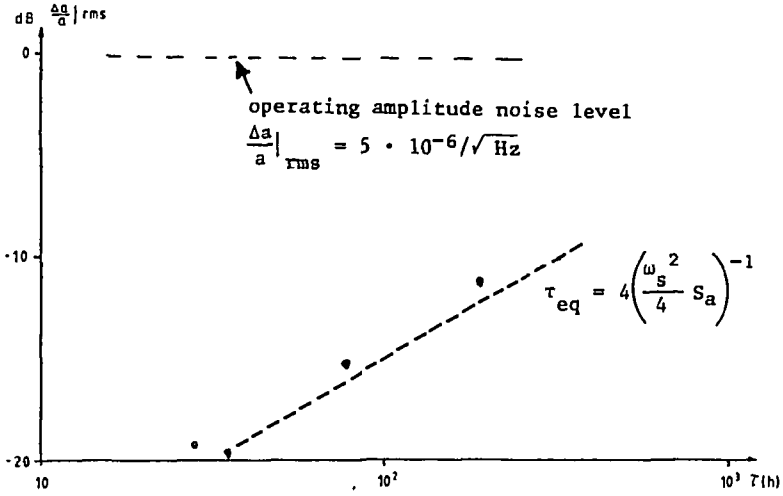

Fig. 23 - Amplitude noise versus equilibrium lifetime in the SPS.

As a first approximation [for $(\omega_s - \omega)$ not too small], take $B(\omega) = j\omega/(\omega_s^2 - \omega^2)$, (s = 0, no synchrotron frequency spread). The phase noise spectrum seen by the beam S_ϕ is related to the measured phase discriminator spectrum S_u by

$$S_\phi = S_u \left(\frac{\omega_s^2 - \omega^2}{\omega^2} \right)^2 \tag{28}$$

From the relations $x \simeq k^2$, $k = \sin \hat{\phi}/2$ and $\omega = h(\hat{\phi})$, (synchrotron frequency vs amplitude), we determine the relation:

$$S_\phi = S_u \, g(x)$$

In order to find an easily calculable solution to the diffusion equation we approximate g(x) by $0.04(1 - x)^{-2}$ (Fig. 24), which finally gives:

$$\tau_{eq} = 20.96/(\omega_s^2 \, S_u(\omega_s)) \tag{29}$$

for a constant "electronic noise" spectral density.

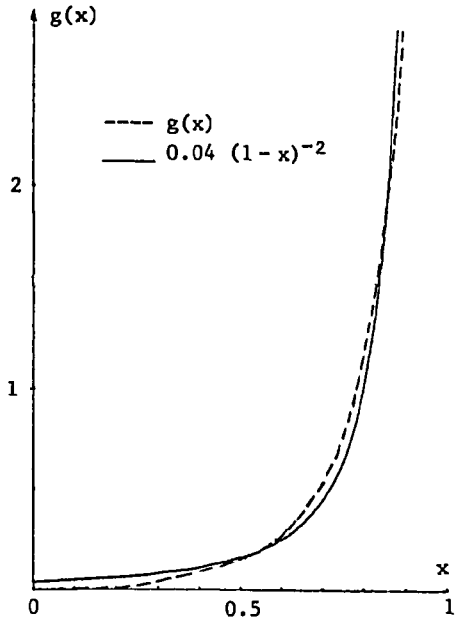

Fig. 24 - Calculated g(x) for a sinusoidal bucket and approximation.

From SPS lifetime measurements, obtained by injecting white noise into the phase loop circuitry, it turns out that this crude estimate is nevertheless very well confirmed by experiment (Fig. 25).

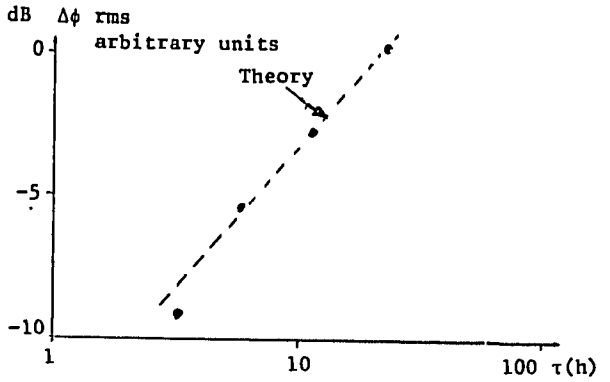

Fig. 25 - RF phase noise versus equilibrium lifetime.

In the case of no phase loop (multibunch case, without individual phase loops, for instance), S_ϕ has a white spectrum and the calculation is easier. There again, the agreement between experiments and theory is satisfactory[24].

When an harmonic cavity is used together with the fundamental RF frequency, the phase space structure, as well as the function $B(\omega)$, becomes more complicated. However, in principle, an analysis similar to that made for a sinusoidal bucket and in the presence of phase loop, will give a function $g(x)$. This function, which may have poles at $x = 0$ and $x = 1$ (if $f_s = 0$ in the centre) will certainly not differ by orders of magnitude from that displayed in Fig. 24 and therefore τ_{eq} should not be extremely different from the value given by 29.

An experiment, made on the SPS with a 4th harmonic cavity (800 MHz) seems to confirm this picture: for the same S_u, τ_{eq} was multiplied by a factor between 3 and 5.

REFERENCES

1. H.G. Hereward, What are the equations for the phase oscillations in a synchrotron, CERN 66-6.

2. C.G. Lilliequist and K.R. Symon, Deviations from adiabatic behaviour during capture of particles into RF bucket, MURA 491.

3. D.G. Edwards, Theoretical RF trapping behaviour.... CERN MPS/BR, Note 73-17.

4. R. Johnson, S. van der Meer, F. Pedersen, G. Shering, Computer control of RF manipulations in the CERN $\bar{p}$ accumulator, IEEE Trans. on Nucl.Science, NS-30, No. 4, p. 2290.

5. R. Johnson, S. van der Meer, F. Pedersen, Measuring and manipulating an accumulated stack. IEEE Trans. on Nucl. Science, NS 30, No. 4, p. 2123.

6. J.E. Griffin, C. Akenbrandt, J.A. MacLachlan, A. Moretti, Isolated bucket RF systems in the Fermilab Antiproton Facility, IEEE Trans. on Nucl. Science, Vol. NS 30, No. 4, p. 3502.

7. K.R. Symon, A.M. Sessler, Proc. CERN Symposium on High Energy Accelerators, Geneva, No. 1, p.44 (1956).

8. W. Schnell, An estimate of the efficiency of phase displacement acceleration in the ISR, CERN ISR-RF/68-18.

9. E.W. Messerschmid, Dispersion of stacked protons.... CERN ISR-RF/72-28.

10. A. Barlow et al., Instrumentation and beam diagnostics in the ISR., Proc. of the 8th Intern. Conf. on High Energy Accelerators, CERN 1971, p.426.

11. D. Boussard, Mesure de la dispersion d'énergie du faisceau dégroupé dans le PS, CERN MPS/BR/MD 72-9.

12. F. Mills, Stability of phase oscillations under two applied frequencies, BNL Int. AADD 176 (1971).

13. D. Boussard, Y. Mizumachi, Numerical computation of the behaviour of bunches in the azimuthal combination processes, CERN-SPS/ARF Note 79-12.

14. R. Garoby, La recombinaison longitudinale dans le PS, principe et mise en oeuvre pratique, CERN/PS/LR Note 80-9.

15. J. Griffin, J. MacLachlan, A.G. Ruggiero, K. Takayama, Time and momentum exchange for production and collection of intense $\bar{p}$ beams, IEEE Trans. on Nucl. Science, Vol NS 30, No. 4, p.2630.

16. R. Garoby, Une procédure de fabrication de paquets courts dans le PS - CERN. PS/LR Note 79-16.

17. B. Autin, The future of the antiproton accumulator, CERN/PS-AA 83/29.

18. J.E. Griffin, J.A. MacLachlan, A. Moretti, IEEE Trans. on Nucl. Science, Vols NS 30, No. 4, p. 3435.

19. D. Boussard, T.P.R. Linnecar, RF noise performance of the CERN $p\bar{p}$ collider. Proc. 12th Int. Conf. on High Energy Accelerators, FNAL 1983 and CERN SPS/ARF 83-33.

20. F.J. Sacherer, A longitudinal stability criterion for bunched beams. IEEE Trans. on Nucl. Science, Vol NS 20, No. 3, p. 825.

21. H.G. Hereward, Open and closed loop properties of an RF accelerated beam, CERN PS/4497 (1964).

22. W. Schnell, Equivalent circuit analysis of phase-lock beam control systems, CERN 68/27.

23. H.G. Hereward, Second-order effects in beam control systems of acceleration, Proc. 1961, Brookhaven Int. Conference, p. 236.

24. D. Boussard, G. Dôme, C. Graziani, The influence of RF noise on the lifetime of bunched proton beams, Proc. 11th Int. Conf. on High Energy Accelerators, CERN, July 1980, p. 620.

25. S. Hansen, A. Hofmann, E. Peschardt, F. Sacherer, W. Schnell, Longitudinal dilution due to RF noise, IEEE Trans. on Nucl. Science, Vol. NS 24, No. 3, p. 1452.

26. U. Wehrle, The low noise oscillator for $p\bar{p}$, CERN SPS/ARF Note 83-10.

27. D. Boussard, E. Brouzet, R. Cappi, J. Gareyte, Collective effects at very high intensity in the CERN PS, IEEE Trans. on Nucl.Science, Vol NS-26, No. 3, June 1979.

28. Y. Mizumachi, Partial linearization of the RF voltage of a storage ring to reduce bunch diffusion, Proc. 11th Int. Conf. on High Energy Accel., CERN July 1980, p. 615.